Role of the Chemical Interactions of the Agonist in Controlling α-Amino-3-hydroxy-5-methyl-4-isoxazolepropionic Acid Receptor Activation†

Kimberly A. Mankiewicz, Anu Rambhadran, Mei Du, Gomathi Ramanoudjame, and Vasanthi Jayaraman*

Department of Integrative Biology and Pharmacology, University of Texas Health Science Center, Houston, Texas 77030

Received November 2, 2006; Revised Manuscript Received December 1, 2006

ABSTRACT: α-Amino-3-hydroxy-5-methyl-4-isoxazolepropionic acid (AMPA) receptors are the main excitatory neurotransmitter receptors in the mammalian central nervous system. Structures of the isolated ligand binding domain of this receptor have provided significant insight into the large-scale conformational changes, which when propagated to the channel segments leads to receptor activation. However, to establish the role of specific molecular interactions in controlling fine details such as the magnitude of the functional response, we have used a multiscale approach, where changes at specific moieties of the agonists have been studied by vibrational spectroscopy, while large-scale conformational changes have been studied using fluorescence resonance energy transfer (FRET) investigations. By exploiting the wide range of activations by the agonists, glutamate, kainate, and AMPA, for the wild type and Y450F and L650T mutants of the GluR2 subtype, and by using the multiscale investigation, we show that the strength of the interactions at the α-amine group of the agonist with the protein in all but one case tracks the extent of activation. Since the α-amine group forms bridging interactions at the cusp of the ligand binding cleft, this appears to be a critical interaction through which the agonist controls the extent of activation of the receptor.

α-Amino-3-hydroxy-5-methyl-4-isoxazolepropionic acid (AMPA)[1] receptors, members of the ionotropic glutamate receptor family, are the main mediators of fast excitatory synaptic transmission in the mammalian central nervous system. Signal transmission is initiated by binding of glutamate to an extracellular ligand binding domain, which leads to the formation of cation specific transmembrane channels (*1*−*6*). Large-scale expression of the isolated extracellular ligand binding domain (S1S2) has led the way for detailed structural studies of this domain. X-ray (*7*−*10*), nuclear magnetic resonance (NMR) (*4*, *11*−*13*), and vibrational spectroscopic (*14*−*16*) investigations using this soluble protein have provided significant insight into the relationship between structure and function in this subtype.

The structures of S1S2 show a graded cleft closure conformational change upon binding agonists with varying efficacy in the bilobed ligand binding domain (*9*, *10*). The extent of cleft closure induced by a given agonist in most cases exhibits a direct correlation to the extent of activation of the receptor, suggesting that this is one of the possible modes of coupling between the ligand binding domain and opening of the ion channel. Vibrational spectroscopic investigations using the S1S2 protein provide a more detailed view of the specific interactions between the agonist and the extracellular ligand binding domain and their role in the functioning of the receptor. The frequency shifts in the asymmetric carboxylate vibrational mode, which is sensitive to the strength of the noncovalent interactions at this moiety, indicate that partial agonist kainate has stronger interactions between its α-carboxylate group and protein relative to those of full agonists AMPA and glutamate, while the S−H stretching vibration of Cys 425, which is a good probe of the strength of the interactions at the α-amine group of the agonists due to its proximity to this group, indicates interactions between the α-amine group of the ligand and the protein for AMPA and glutamate are stronger than the interactions for kainate. The vibrational studies (*14*, *15*), when placed in the context of the X-ray crystallography (*8*, *9*) and NMR (*4*, *11*−*13*) structures, appear to suggest that stronger interactions at the α-amine group with a concomitant decrease in the strength of the interactions at the α-carboxylate group for a ligand correlate with a greater extent of cleft closure and full agonism. Weaker interactions at the α-amine group accompanied by an increase in the strength of the interactions at the α-carboxylate group for a ligand result in a lower level of cleft closure, as compared to the full agonists, and a partial agonist response. Using this background on the wild-type proteins (*14*, *15*), here we have studied the role of the interactions between the agonist and protein in more detail by using the Y450F and L650T mutants that provide a wide range of activations for the three agonists glutamate,

† This work was supported by National Science Foundation Grant MCB-04444352, National Institutes of Health Grants R21NS051378, R03AA015682-01, and R01GM073102, and the Muscular Dystrophy Association. K.A.M. was supported by National Institutes of Health Molecular Biophysics Training Grant T32 GM008280.

* To whom correspondence should be addressed: Department of Integrative Biology and Pharmacology, University of Texas Health Science Center, 6431 Fannin St., Houston, TX 77030. Telephone: (713) 500-6236. Fax: (713) 500-7444. E-mail: vasanthi.jayaraman@uth.tmc.edu.

[1] Abbreviations: AMPA, α-amino-3-hydroxy-5-methyl-4-isoxazolepropionic acid; GluR2, glutamate receptor subunit 2; GluR4, glutamate receptor subunit 4; FRET, fluorescence resonance energy transfer; FTIR, Fourier transform infrared; NMR, nuclear magnetic resonance.

10.1021/bi062270l CCC: $37.00
Published on Web 01/18/2007

kainate, and AMPA, thus allowing for detailed comparisons of the specific ligand−protein interactions, cleft closure, and activation in deducing the relationship among these three factors in receptor function.

The Y450 residue is conserved among all AMPA and kainate receptors, and the L650 residue is conserved among all AMPA receptors and is replaced with a valine in kainate receptors (*17*). Crystal structures of the kainate-bound form of the GluR2-S1S2 protein suggest that the kainate is sterically hindered by the Y450 and L650 residues, allowing only for partial cleft closure in the GluR2-S1S2 protein (*9*, *18*). This steric hindrance is thought to be one of the reasons why kainate is a partial agonist. This hypothesis is strengthened by the fact that electrophysiological investigations of the Y450A or -W and L650T or -V mutations, which are expected to either introduce more flexibility into the ligand binding domain at the Y450 site or decrease the size of the L650 residue, show an increase in the level of kainate activation (*18*−*20*). X-ray structures are available for the kainate-bound forms of the Y450W (*19*) and L650T (*18*) mutants, and these structures show that the increase in the extent of activation is accompanied by an increase in the degree of cleft closure relative to the degree of cleft closure observed in the kainate-bound form of the wild-type S1S2 protein. The AMPA- and glutamate-bound forms of the L650T mutant, on the other hand, do not follow the same trends as the wild-type protein, and on average, the AMPA-bound state of the mutant is more closed than the glutamate-bound state while the level of activation by AMPA is significantly lower than that by glutamate (*18*, *20*). Since in this mutant the cleft closure versus activation correlation is the reverse of that observed in the wild-type protein, the mechanism that dictates the subtleties of the differences in activation between AMPA and glutamate for this mutant protein is still largely unknown.

Here we have performed a multiscale analysis where the changes in the specific interactions are correlated with the cleft closure conformational changes as well as receptor activation using the Y450F and L650T mutants with the goal of understanding the role of the agonist−protein interactions in mediating the cleft closure conformational changes and receptor activation. The Y450F mutation was chosen instead of the Y450W or Y450A mutations since the Y450F-S1S2 protein is relatively more stable than Y450W-S1S2 or Y450A-S1S2. The activation profile as well as the extent of cleft closure has previously been reported for the L650T mutant (*18*, *20*), and hence, here we have determined the activation profile and extent of cleft closure for the Y450F mutation for the three agonists glutamate, kainate, and AMPA. Additionally, vibrational spectra were obtained for the three agonists bound to the Y450F-S1S2 and L650T-S1S2 proteins.

MATERIALS AND METHODS

Preparation and Purification of Y450F-S1S2 and L650T-S1S2. The S1S2J plasmid was generously provided by E. Gouaux (Oregon Health and Sciences University, Portland, OR). The Y450F and L650T mutations were introduced using the QuikChange site-directed mutagenesis kit (Stratagene). The Y450F and L650T mutants of GluR2-S1S2 (Y450F-S1S2 and L650T-S1S2) were expressed and purified as previously detailed (*18*). In brief, the plasmids were expressed in *Escherichia coli* Origami B(DE3) cells. After centrifugation and clarification, the protein was purified on a Ni-NTA HiTrap column (GE Healthcare Life Sciences). The His tag was removed by thrombin digestion and further purified using a SP-Sepharose column (GE Healthcare Life Sciences).

The binding properties of the wild-type and Y450F-S1S2 proteins were determined by measuring the tryptophan fluorescence as outlined by Cheng et al. (*21*). The K_d values determined by these fluorescence measurements for the binding of AMPA, glutamate, and kainate to the wild-type and Y450F mutant S1S2 proteins are listed in Table 1 of the Supporting Information.

Fluorophore Labeling. Protein (0.5 μM) in phosphate-buffered saline with 1 mM glutamate (Sigma-Aldrich) was labeled with a 1:1 ratio of the malemide derivatives of fluorescein (Biotium, Hayward, CA) and diethylenetriaminepentaacetic acid chelate of terbium (DTPA-Tb) (Invitrogen). The protein was then dialyzed extensively against phosphate-buffered saline and used for FRET measurements.

Fluorescence Measurements. Fluorescence measurements were taken using a TimeMaster model TM-3/2003 instrument (Photon Technologies, Inc., Lawrenceville, NJ). The energy source was a nitrogen laser system coupled by a fiber optic to the sample compartment. The scattered light was passed through a monochromator to a stroboscopic detector. Data were collected using Felix 32 (Photon Technologies, Inc.) and analyzed with Origin (OriginLab Corp., Northampton, MA). The fluorescence data were obtained with at least two to three different protein samples, and for each sample, the data were an average of five shots (hence, the data shown are an average of 10−15 data points). The data from each independent sample were also fit to ensure that there were no significant differences between samples of the same protein.

Distance Calculations Based on Lifetime Measurements. The distance between the donor and acceptor fluorophores was determined by measuring the time constants of the donor fluorescence decay in the absence of the acceptor (τ_D) and the sensitized emission of the acceptor as a result of energy transfer from the donor (τ_{DA}). The distance was then determined using eq 1 given by Förster's theory of energy transfer:

$$R = R_0\left(\frac{\tau_{DA}}{\tau_D - \tau_{DA}}\right)^{1/6} \quad (1)$$

R_0 was calculated using the overlap integral as described previously (*20*, *22*).

FTIR Difference Spectroscopy. The same protocol was used to collect the FTIR data as outlined in detail in refs *14*, *15*, and *23*. Protein (500 μM) in 25 mM phosphate buffer containing 250 mM NaCl and 0.02% NaN_3 (pH 7.4) was used for the measurements shown in Figure 3, and 1 mM protein in 10 mM HEPES buffer containing 100 mM NaCl (pH 7.4) was used for the measurements shown in Figure 4. D_2O was used as the solvent to obtain spectra in the 1450−1800 cm^{-1} range due to the large infrared absorption of water at $\approx$1600 cm^{-1}. Water was used as the solvent to study the S−H stretching vibration. In all cases, excess ligand concentrations ($\geq$10 mM) were used. The presence of excess

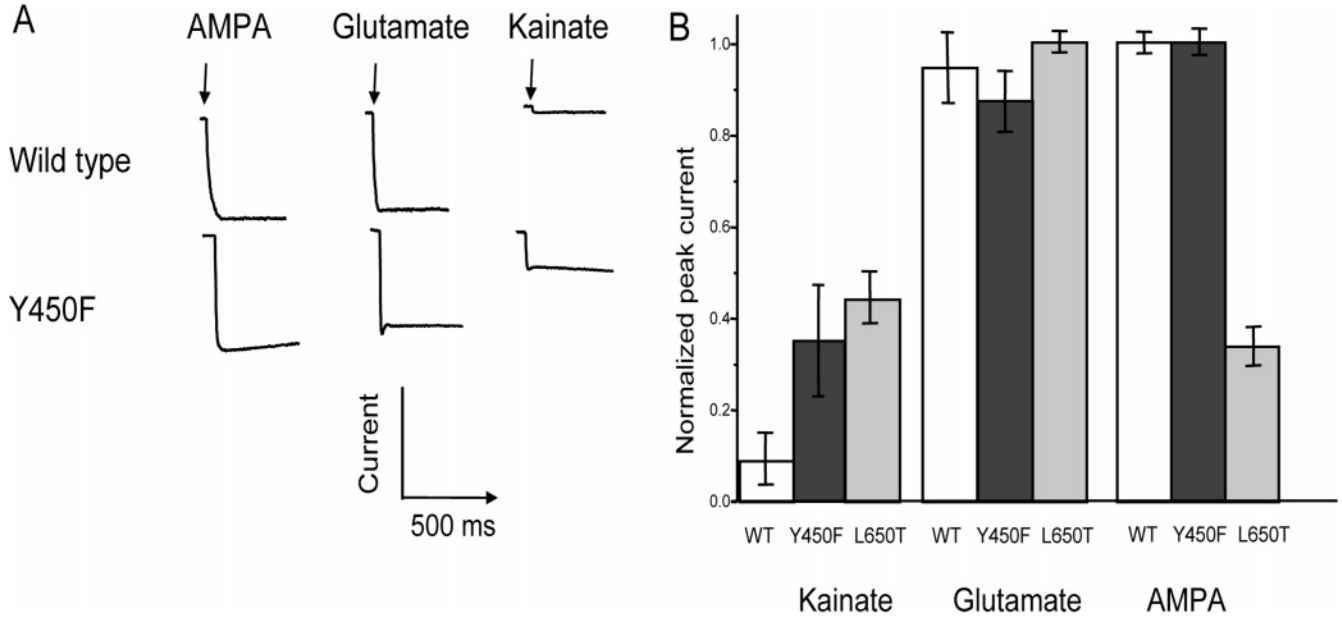

FIGURE 1: Electrophysiology for the wild type and Y450F. (A) Whole cell current recordings of the wild type and Y450F expressed in HEK 293 cells resulting from exposure to 10 mM glutamate, 10 mM kainate, and 5 mM AMPA with 100 μM cyclothiazide. (B) Maximum currents resulting from glutamate, AMPA, and kainate normalized to the currents mediated by 10 mM AMPA for the wild type and Y450F and to 10 mM glutamate for L650T.

unbound ligand was confirmed by the bands arising from unbound ligands in all the spectra that were recorded. Peaks from unbound agonists were subtracted using a spectrum of the agonist in buffer.

FTIR spectra were obtained using a Nicolet Nexus 870 spectrometer. An adjustable path length infrared cell holder (Aldrich) was used to record the spectra. Spectra were collected at 4 cm^{-1} resolution at a constant temperature of 15 °C. A path length of 50 μm was used to obtain the spectra in the 1450−1800 cm^{-1} range, while a path length of 75 μm was used to investigate the S−H stretching. Difference spectra were obtained by subtracting the unligated form of the protein from the ligated form of the protein. Collection and manipulation of data were performed using Omnic and GRAMS/AI (7.01) (Thermoelectron, Waltham, MA).

Electrophysiological Measurements. The GluR2-flip plasmid was kindly provided by Dr. Seeburg (Max Planck Institute, Heidelberg, Germany). The Y450F point mutation was introduced into the plasmid using the Stratagene QuikChange site-directed mutagenesis kit (Stratagene), and the final construct was verified by sequencing the coding region of the DNA. For the electrophysiological measurements, the wild-type and mutant receptors were expressed in human embryonic kidney 293 (HEK 293) cells (ATCC CRL 1573) using the same protocol that was outlined by Madden et al. (*24*). Briefly, the cells were cultured in DMEM supplemented with 10% fetal bovine serum (Life Technologies, Bethesda, MD), and transfections were performed using Fugene 6 (Roche, Indianapolis, IN) transfection reagent, with 1−2 μg of glutamate receptor cDNA and 0.5 μg of plasmid containing the cDNA for green fluorescent protein. Cells were used 2−4 days after transfection.

For whole cell current recordings, transfected HEK 293 cells were voltage-clamped at a holding potential of −60 mV, and solutions were applied using a homemade U-tube mixing device that had a 100 μm aperature. The electrode solution, for the electrophysiological measurements, contained 140 mM $CaCl_2$, 2 mM $MgCl_2$, 1 mM $CaCl_2$, 10 mM EGTA, 2 mM Na_2ATP, and 10 mM HEPES (pH 7.4). The extracellular bath solution contained 145 mM NaCl, 1.8 mM $MgCl_2$, 3 mM KCl, 10 mM glucose, and 10 mM HEPES (pH 7.4). Currents were amplified with an Axon 200B amplifier (Molecular Devices, Sunnyvale, CA), low-pass-filtered at 1 kHz. The filtered signal was digitized using a Labmaster DMA digitizing board controlled by Axon PClamp. All the experiments were performed at room temperature.

RESULTS AND DISCUSSION

Functional Properties. Whole cell currents due to the activation of wild-type and Y450F GluR2-flip receptors expressed in HEK 293 cells are shown in Figure 1A. The whole cell currents were mediated by saturating concentrations of glutamate (10 mM), AMPA (5 mM), and kainate (10 mM) under non-desensitizing conditions in the presence of 100 μM cyclothiazide. To assess the relative activations by the three agonists, the average maximum peak currents were normalized to the currents mediated by 10 mM AMPA (Figure 1B). As previously reported, for the wild-type receptor, kainate-mediated currents are approximately 10% of the currents mediated by full agonists glutamate and AMPA (*20*). In contrast, kainate mediates significantly larger currents upon binding to the Y450F mutant, producing approximately 37% of the currents mediated by AMPA, indicating that the activation by kainate is stronger in the Y450F mutant than in the wild-type receptor. Additionally, a slight decrease is observed in the extent of activation by glutamate in the Y450F mutant relative to the extent of activation in the wild-type receptor, from 95 to 87% activation relative to the currents mediated by AMPA. The whole cell currents mediated by L650T have been reported previously (*20*) and are provided in Figure 1B for comparison. Kainate activation at this mutant is stronger than that

Table 1: Lifetime Measurements for Y450F-S1S2[a]

ligated state	τ_D (μs)	τ_{DA} (μs)
apo	1565 ± 23	242 ± 2.7
glutamate	1515 ± 15	140 ± 1.7
AMPA	1515 ± 13	131 ± 1.8
kainate	1543 ± 19	166 ± 2.0

[a] Fluorescence lifetimes for Y450F-S1S2 (T394C;S652C) tagged with terbium chelate (τ_D) and Y450F-S1S2 (T394C;S652C) tagged with a 1:1 ratio of terbium chelate and fluorescein (τ_{DA}).

in the wild-type protein, while activation by AMPA is significantly weaker.

The stronger activation of the Y450F mutant by kainate relative to that of the wild-type receptors is consistent with the expectation that the Y450F mutation would introduce more flexibility in the ligand binding pocket due to the loss of hydrogen bonding interactions, possibly decreasing the steric hindrance by the Y450 residue that interferes with kainate binding. The decrease in steric hindrance in the Y450F mutant not only increases the extent of activation by kainate but also, consistent with the fact that kainate is able to make better interactions with the protein, increases the affinity for kainate slightly, with the K_d for kainate decreasing from 800 nM for the wild-type protein to 600 nM for the Y450F mutant (Table 1 of the Supporting Information). To determine if the flexibility in the cleft allows for a larger cleft closure by kainate in the Y450F ligand binding domain relative to the wild-type protein, we have used a FRET-based probe that provides a readout of the extent of cleft closure.

Extent of Cleft Closure. Here Y450F-S1S2 is tagged with donor and acceptor fluorophores at position 394 in domain 1 and position 652 in domain 2. Since the donor and acceptor are tagged at sites that reflect the cleft closure conformational changes, the distances as measured by FRET provide a direct readout of the extent of cleft closure (*20*).

The lifetimes for the donor only and donor−acceptor tagged Y450F-S1S2 mutant protein in the apo form and the glutamate-, AMPA-, and kainate-bound forms are listed in Table 1 along with the errors associated with the fits (data are shown in Figure 1 of the Supporting Information). No changes are observed in the donor only lifetimes between the apo and various ligated states, while binding of the ligands results in a difference in the FRET-sensitized lifetimes in the donor−acceptor tagged samples in the following order: glutamate ≈ AMPA < kainate < apo. These lifetime measurements indicate that the distance between the donor and acceptor decreases from the apo state to the ligated states, with glutamate and AMPA binding inducing a larger decrease in the distance between the donor and acceptor than kainate.

The distances determined by FRET for Y450F-S1S2 are plotted as a function of the extent of activation for the three agonists kainate, AMPA, and glutamate and compared with the previously reported results for wild-type S1S2 and L650T-S1S2 (*20*) in Figure 2. The distance between the donor and acceptor for the AMPA-bound state of Y450F-S1S2 is comparable to that of the AMPA-bound form of the wild-type protein. This indicates similar cleft closure in the two proteins upon binding of AMPA. The distance between the donor and acceptor is slightly larger for the glutamate-bound form of Y450F-S1S2 than for the glutamate-bound form of the wild-type receptor, while the kainate-bound form

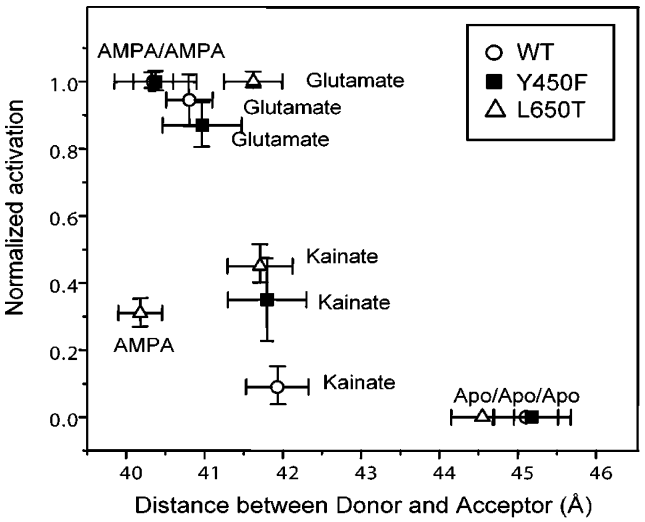

FIGURE 2: Cleft closure in the wild type, Y450F-S1S2, and L650T-S1S2. Distances between T394C and S652C as measured by fluorescence resonance energy transfer for the wild type (○), Y450F-S1S2 (■), and L650T-S1S2 (△) are plotted as a function of the extent of activation.

of Y450F-S1S2 exhibits a distance between the donor and acceptor slightly shorter that that of the kainate-bound form of the wild-type protein. However, these changes are within the error of the measurements and hence not significant. The changes in the distance between the different agonist-bound forms of Y450F-S1S2, on the other hand, are significantly larger than the error associated with the measurements, and these distance changes show that Y450F-S1S2 follows the same trends as the wild-type protein with a direct correlation between the extent of cleft closure and the amount of activation.

The L650T mutant on the other hand, as previously reported (*20*), does not follow the same trends as the wild type and Y450F mutant. AMPA, a partial agonist of this mutant protein, exhibits a larger extent of cleft closure, while glutamate, which induces larger currents than AMPA does, has a relatively more open cleft (Figure 2).

Agonist Environment in Wild-Type and Mutant Proteins. The FTIR difference spectra between the agonist-bound and unligated forms of the wild-type, Y450F-S1S2, and L650T-S1S2 proteins, in the region of 1560−1740 cm^{-1}, are shown in Figure 3. As reported previously, this region of the FTIR spectrum has modes due to the carboxylate/isoxazole moieties of the agonists, as well as the amide I vibrations from the protein backbone (*14*, *15*). The asymmetric stretching vibration of the α-carboxylate is assigned using ^{13}C labeling at the α-carboxylate position for AMPA and glutamate, while the other features are assigned on the basis of frequencies.

Secondary Structure Changes. The amide I feature at 1630 cm^{-1} for the glutamate and AMPA difference spectra, and at 1625 cm^{-1} for the kainate difference spectra, can be assigned on the basis of frequency to changes at β-sheets (*14*). The difference feature at this frequency is upshifted in the Y450F difference spectrum relative to the wild-type difference spectrum for all the agonists, while exhibiting slight upshifts or no changes in the L650T difference spectra for the three agonists relative to the wild-type spectra. This trend in the extent of upshift has no specific correlation to the extent of changes in the activation or to the extent of

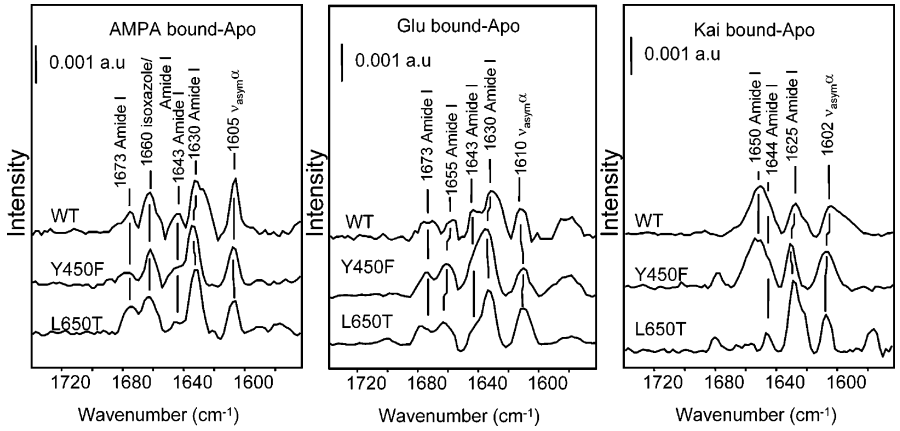

FIGURE 3: Changes at the α-carboxylate and secondary structural modes. Difference FTIR spectra in the region of 1560−1740 cm^{-1} between agonist-bound wild-type S1S2 and unligated S1S2, agonist-bound Y450F-S1S2 and unligated Y450F-S1S2, and agonist bound L650T-S1S2 and unligated L650T-S1S2 for the three agonists AMPA, glutamate, and kainate.

cleft closure and therefore most likely reflects the local perturbation due to the mutations, since similar trends are observed for a given mutation. Specifically, the larger upshifts for the Y450F mutation could arise from the larger flexibility expected for this mutant due to the loss of the hydrogen bonding network contribution of the tyrosine residue. This correlation would also be consistent with the lack of large changes in the L650T mutation, which is not expected to cause a large change in the flexibility and dynamics.

The amide I feature at 1643/1644 cm^{-1}, on the other hand, appears to show a correlation to the extent of activation. The intensity of this feature is significantly lower in the difference spectrum due to binding of AMPA and kainate to L650T-S1S2 relative to the intensity of this feature in the difference spectrum due to binding of a full agonist (AMPA and glutamate) to the wild-type protein. This decrease in intensity correlates to a decrease in extent of activation of the receptor. Additionally, in the kainate-induced difference spectra for the Y450F mutant as well as the wild type, a new band with significantly higher intensity is observed at 1650 cm^{-1}. It should also be noted that although AMPA activation of the L650T mutation and kainate activation of the Y450F mutation are similar, the difference features due to binding of AMPA to L650T-S1S2 and binding of kainate to Y450F-S1S2 are different. This indicates that although the same trends in the changes at the 1643/1644 cm^{-1} feature are observed for both kainate and AMPA binding, the exact correlations between changes at the 1643/1644 cm^{-1} feature and activation differ for the different agonists. This could arise due to subtle differences in the mechanisms of activation between these two agonists. The 1643/1644 cm^{-1} frequency indicates that this feature can arise due to changes in random structures, irregular β-sheets, and/or solvent-exposed helices (*14*, *25*). Hence, this feature cannot be assigned to a specific conformational change, but for a given agonist, the intensity appears to correlate to the extent of agonism. However, it would be necessary to study a series of agonists to determine if this feature is indeed a diagnostic tool of the extent of agonism.

Environment of the Agonist: Interactions at the α-Carboxylate. The frequency of the asymmetric carboxylate vibration of the α-carboxylates of the agonists has previously been shown to be a probe of the strength of the noncovalent interactions between this moiety and the protein (*14*, *15*). A downshift in this feature is indicative of a relatively more favorable interaction, and conversely, an upshift suggests more unfavorable interactions.

In the difference spectrum showing the asymmetric α-carboxylate vibrations (Figure 3), no significant changes are observed in the frequency of the asymmetric α-carboxylate vibrations for AMPA and glutamate between the wild-type proteins and mutant proteins. A 1 cm^{-1} downshift is observed in the L650T-S1S2 protein for AMPA and a 1 cm^{-1} downshift in the Y450F-S1S2 protein for glutamate relative to their frequencies in the wild-type proteins. This indicates that the strengths of the noncovalent interactions between the α-carboxylates and protein may be slightly more favorable for AMPA in the L650T mutant and for glutamate in the Y450F mutant than those in the wild-type protein. The largest changes are observed in the kainate-induced difference features, where 4 and 5 cm^{-1} upshifts are observed in the frequencies of this mode in the Y450F-S1S2 and L650T-S1S2 difference spectra, respectively, relative to the frequency of this mode when kainate is bound to the wild-type protein. This indicates a significantly less favorable and weaker interaction at the α-carboxylate of kainate with the Y450F and L650T mutants relative to its interaction with the wild-type protein (*14*, *15*).

Cysteine 425 Environment: Probe of the Strength of the Interactions at the α-Amine Group of the Ligand. Since the α-amine group of the agonist is hydrogen bonded to Pro 478, and the backbone of the adjacent residue, Ala 477, is hydrogen bonded to Cys 425 (*9*), changes in the strength of the hydrogen bond at Cys 425 as probed by the S−H stretching vibration are expected to reflect changes in the interaction between the α-amine group of the agonist and the protein. It should be noted that the GluR2-S1S2 protein has two non-disulfide-bonded cysteines, Cys 436 and Cys 425. However, Cys 436 is far from the ligand binding site, and the S−H stretching vibration of this residue does not change between the various ligated states (*14*). Thus, the difference spectrum between the agonist and apo state reflects changes in the frequency of the S−H stretch of Cys 425. This has been further verified by studies with GluR4-S1S2 which contains a single non-disulfide-bonded cysteine that is at the Cys 425 position (position 426 in GluR4) (*14*, *15*).

In the difference spectra in the region of the S−H stretching mode (Figure 4), the difference spectra are

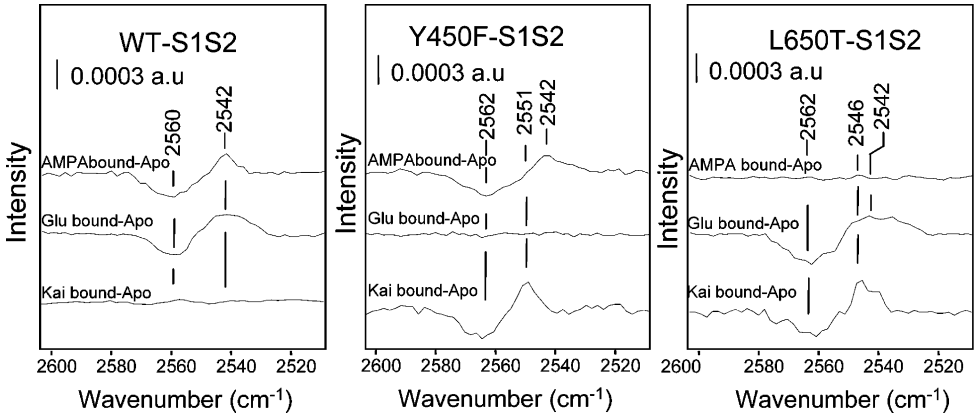

FIGURE 4: Changes at the Cys 425 S−H stretching mode. Difference FTIR spectra in the region of 2500−2600 cm^{-1} between agonist-bound wild-type S1S2 and apo S1S2, agonist-bound Y450F-S1S2 and apo Y450F-S1S2, and agonist-bound L650T-S1S2 and apo L650T-S1S2 for the three agonists AMPA, glutamate, and kainate.

obtained between the agonist and apo state; hence, the positive band corresponds to the frequency of the S−H stretching vibration of Cys 425 in the bound state, while the negative band corresponds to its frequency in the apo state. In the wild-type protein, both AMPA and glutamate induce a large 18 cm^{-1} downshift in the S−H stretch relative to that in the apo state, while kainate has no effect. This downshift indicates a stronger hydrogen bond at Cys 425 upon binding of AMPA and/or glutamate relative to that in the apo state and can be attributed to strong interactions between the α-amine group of AMPA and/or glutamate and the protein, while the lack of changes due to kainate binding suggests weak interactions at the α-amine group of kainate with the protein (*14*). Along the same lines, in the case of the Y450F mutant, the shifts follow the order AMPA > kainate > glutamate, which would imply that the strength of the interactions follows the order AMPA > kainate > glutamate, and in the case of the L650T mutation, the shifts follow the order glutamate > kainate > AMPA, which would imply that the strength of the interactions follows the same order.

Tug of War between the α-Carboxylate and the α-Amine Group of the Ligand. In the case of the wild-type protein, the strength of the interactions at the α-carboxylate of the ligand follows the order kainate > AMPA > glutamate, which has an inverse correlation to the changes in the strength of the interactions at the α-amine group that follows the order glutamate ≈ AMPA > kainate (*14*). Similar trends are seen for kainate-induced differences between the mutant and wild-type protein (Table 2), where a large downshift in the S−H stretching vibrational frequency between the kainate and apo forms of the protein is accompanied by a smaller downshift of the asymmetric stretching vibrational band of the α-carboxylate in the protein relative to the unbound. This would be consistent with the observation in the wild-type protein where an increase in the strength of the interactions at the α-amine group is accompanied by a decrease in the strength of the interactions at the α-carboxylate. Binding of AMPA and glutamate to the proteins yields smaller shifts in the α-carboxylate vibrational mode as a result of larger changes at the α-amine group relative to those observed for kainate (Table 2). This could be a reflection of the larger steric constraints of kainate in the AMPA receptor binding site relative to AMPA and glutamate. Although the magnitude of the changes at the α-carboxylate vibrational mode is different for the three agonists glutamate, AMPA, and kainate, similar trends, where an increase in the strength of the interactions at the α-amine group results in a decrease in the strength of the interactions at the α-carboxylate, are observed for all the agonists in both the wild type and the two mutant proteins.

Table 2: Frequency Shifts for the Wild Type, Y450F-S1S2, and L650T-S1S2[a]

protein−agonist	α-carboxylate shift (cm^{-1})	S−H shift (cm^{-1})
wild type−AMPA	9	18
Y450F−AMPA	9	20
L650T−AMPA	10	0
wild type−glutamate	4	18
Y450F−glutamate	5	0
L650T−glutamate	4	20
wild type−kainate	18	0
Y450F−kainate	14	11
L650T−kainate	13	16

[a] Shift in the frequency of the α-carboxylate asymmetric stretching vibration of the agonist bound to the protein relative to its frequency in buffer and of the Cys 425 S−H stretching vibration in the agonist-bound state relative to the apo state.

Correlation among Ligand Environment, Cleft Closure, and Activation in the Glutamate Receptor. The vibrational spectra, with the exception of binding of glutamate to Y450F, show a correlation between the strength of the interactions at the α-amine group and the level of activation of the receptor such that a stronger interaction at the α-amine group results in a larger level of activation of the channel. The L650T mutation in particular is interesting because in this mutant the extent of cleft closure upon agonist binding does not exhibit the same correlation to the extent of activation as seen in the wild type and other mutant proteins (*20*). Here, we show that while the extent of cleft closure does not correlate to the degree of activation in the L650T mutant, the strength of the interactions at the α-amine group follows the same trend in this mutant as in the wild type and the AMPA- and kainate-bound forms of the Y450F mutant. Hence, AMPA, a partial agonist at this mutant, has weak interactions at the α-amine group, while glutamate, a full agonist at this mutant, exhibits stronger interactions at the α-amine group. These results suggest that the interactions between the α-amine group of the agonist and the protein

are an important point of communication between the agonist and protein and an important player in the allosteric pathway of agonist-induced receptor activation.

The only exception to the correlation between the shift in the S−H stretching frequency and the degree of activation is the glutamate-bound form of the Y450F mutant. In this case, glutamate is a full agonist and yet shows a lack of change at the S−H stretching vibration. The lack of a change at the S−H stretching vibration could result from the greater flexibility in this mutant due to the loss in the hydrogen bonding network on the domain 1 side of the cleft, resulting in a loss of the correlation between changes at Cys 425 and the strength of interactions at the α-amine group of glutamate, and/or it is also possible that the lack of a shift in the S−H frequency reflects weak interactions at the α-amine group of glutamate and that glutamate activation of this mutant is controlled by a different mechanism involving other controls that mediate agonist-induced activation. It is important to note that the extent of cleft closure for glutamate activation of the Y450F mutant follows the same trends as that observed for the wild-type protein (Figure 2). Thus, it is possible that in this mutant the conformational change plays the primary role in mediating the activation of the receptor. On the other hand, since the dynamics of this protein are altered by the Y450F mutation, due to the loss in the hydrogen bonding network, the interactions at the α-amine group may no longer be critical and the activation could be controlled by subtle changes in the dynamics. This mutant would hence be a good candidate for future NMR investigations where the role of the differences in dynamics with respect to differences in activation can be studied.

The large number of X-ray structures of the isolated ligand binding domain in complex with various agonists (*7*, *9*, *10*, *18*) clearly indicate that the cleft closure conformational change plays an important role in mediating agonist-induced receptor activation in the glutamate receptor. The breakdown in the correlation between the extent of cleft closure and activation for L650T-S1S2, however, suggests that in addition to the cleft closure conformation, subtle differences in the extent of activation could be controlled by other mediators. Here we show that the strength of interactions at the α-amine group of the agonist could be one such mediator since in eight of the nine cases that were studied the extent of the interactions at this moiety correlates to the extent of activation.

SUPPORTING INFORMATION AVAILABLE

K_d values for binding of AMPA, glutamate, and kainate to wild-type GluR2-S1S2 and Y450F-S1S2 (Table 1) and excited state lifetimes for Y450F-S1S2 (Figure 1). This material is available free of charge via the Internet at http://pubs.acs.org.

REFERENCES

1. Hollmann, M., and Heinemann, S. (1994) Cloned glutamate receptors, *Annu. Rev. Neurosci. 17*, 31−108.
2. Dingledine, R., Borges, K., Bowie, D., and Traynelis, S. F. (1999) The glutamate receptor ion channels, *Pharmacol. Rev. 51*, 7−61.
3. Madden, D. R. (2002) The structure and function of glutamate receptor ion channels, *Nat. Rev. Neurosci. 3*, 91−101.
4. McFeeters, R. L., and Oswald, R. E. (2004) Emerging structural explanations of ionotropic glutamate receptor function, *FASEB J. 18*, 428−438.
5. Oswald, R. E. (2004) Ionotropic glutamate receptor recognition and activation, *Adv. Protein Chem. 68*, 313−349.
6. Mayer, M. L. (2006) Glutamate receptors at atomic resolution, *Nature 440*, 456−462.
7. Jin, R., Horning, M., Mayer, M. L., and Gouaux, E. (2002) Mechanism of activation and selectivity in a ligand-gated ion channel: Structural and functional studies of GluR2 and quisqualate, *Biochemistry 41*, 15635−15643.
8. Armstrong, N., Sun, Y., Chen, G. Q., and Gouaux, E. (1998) Structure of a glutamate-receptor ligand-binding core in complex with kainate, *Nature 395*, 913−917.
9. Armstrong, N. A., and Gouaux, E. (2000) Mechanisms for activation and antagonism of an AMPA-sensitive glutamate receptor: Crystal structures of the GluR2 ligand binding core, *Neuron 28*, 165−181.
10. Jin, R., Banke, T. G., Mayer, M. L., Traynelis, S. F., and Gouaux, E. (2003) Structural basis for partial agonist action at ionotropic glutamate receptors, *Nat. Neurosci. 6*, 803−810.
11. McFeeters, R. L., and Oswald, R. E. (2002) Structural mobility of the extracellular ligand-binding core of an ionotropic glutamate receptor. Analysis of NMR relaxation dynamics, *Biochemistry 41*, 10472−10481.
12. McFeeters, R. L., Swapna, G. V., Montelione, G. T., and Oswald, R. E. (2002) Semi-automated backbone resonance assignments of the extracellular ligand-binding domain of an ionotropic glutamate receptor, *J. Biomol. NMR 22*, 297−298.
13. Valentine, E. R., and Palmer, A. G., III (2005) Microsecond-to-millisecond conformational dynamics demarcate the GluR2 glutamate receptor bound to agonists glutamate, quisqualate, and AMPA, *Biochemistry 44*, 3410−3417.
14. Cheng, Q., and Jayaraman, V. (2004) Chemistry and conformation of the ligand-binding domain of GluR2 subtype of glutamate receptors, *J. Biol. Chem. 279*, 26346−26350.
15. Jayaraman, V., Keesey, R., and Madden, D. R. (2000) Ligand−protein interactions in the glutamate receptor, *Biochemistry 39*, 8693−8697.
16. Cheng, Q., Du, M., Ramanoudjame, G., and Jayaraman, V. (2005) Evolution of glutamate interactions during binding to a glutamate receptor, *Nat. Chem. Biol. 1*, 329−332.
17. Pentikainen, O. T., Settimo, L., Keinanen, K., and Johnson, M. S. (2003) Selective agonist binding of (S)-2-amino-3-(3-hydroxy-5-methyl-4-isoxazolyl)propionic acid (AMPA) and 2S-(2α,3β,4β)-2-carboxy-4-(1-methylethenyl)-3-pyrrolidineacetic acid (kainate) receptors: A molecular modeling study, *Biochem. Pharmacol. 66*, 2413−2425.
18. Armstrong, N., Mayer, M., and Gouaux, E. (2003) Tuning activation of the AMPA-sensitive GluR2 ion channel by genetic adjustment of agonist-induced conformational changes, *Proc. Natl. Acad. Sci. U.S.A. 100*, 5736−5741.
19. Holm, M. M., Naur, P., Vestergaard, B., Geballe, M. T., Gajhede, M., Kastrup, J. S., Traynelis, S. F., and Egebjerg, J. (2005) A binding site tyrosine shapes desensitization kinetics and agonist potency at GluR2. A mutagenic, kinetic, and crystallographic study, *J. Biol. Chem. 280*, 35469−35476.
20. Ramanoudjame, G., Du, M., Mankiewicz, K. A., and Jayaraman, V. (2006) Allosteric mechanism in AMPA receptors: A FRET-based investigation of conformational changes, *Proc. Natl. Acad. Sci. U.S.A. 103*, 10473−10478.
21. Cheng, Q., Thiran, S., Yernool, D., Gouaux, E., and Jayaraman, V. (2002) A vibrational spectroscopic investigation of interactions of agonists with GluR0, a prokaryotic glutamate receptor, *Biochemistry 41*, 1602−1608.
22. Du, M., Reid, S. A., and Jayaraman, V. (2005) Conformational changes in the ligand-binding domain of a functional ionotropic glutamate receptor, *J. Biol. Chem. 280*, 8633−8636.
23. Jayaraman, V. (2004) Spectroscopic and kinetic methods for ligand-protein interactions of glutamate receptor, *Methods Enzymol. 380*, 170−187.
24. Madden, D. R., Cheng, Q., Thiran, S., Rajan, S., Rigo, F., Keinanen, K., Reinelt, S., Zimmermann, H., and Jayaraman, V. (2004) Stereochemistry of glutamate receptor agonist efficacy: Engineering a dual-specificity AMPA/kainate receptor, *Biochemistry 43*, 15838−15844.
25. Chapman, D., Jackson, M., and Haris, P. I. (1989) Investigation of Membrane-Protein Structure Using Fourier-Transform Infrared-Spectroscopy, *Biochem. Soc. Trans. 17*, 617−619.

BI062270L